Review in Advance first posted online on October 5, 2012. (Changes may still occur before final publication online and in print.)

Analysis of Fluid Flows via Spectral Properties of the Koopman Operator

Igor Mezić

Department of Mechanical Engineering, University of California, Santa Barbara, California 93106; email: mezic@engineering.ucsb.edu

Annu. Rev. Fluid Mech. 2013. 45:357–78

The *Annual Review of Fluid Mechanics* is online at fluid.annualreviews.org

This article's doi: 10.1146/annurev-fluid-011212-140652

0066-4189/13/0115-0357$20.00

Keywords

Koopman mode expansion, dynamic mode decomposition, global modes, Arnoldi algorithm

Abstract

This article reviews theory and applications of Koopman modes in fluid mechanics. Koopman mode decomposition is based on the surprising fact, discovered in Mezić (2005), that normal modes of linear oscillations have their natural analogs—Koopman modes—in the context of nonlinear dynamics. To pursue this analogy, one must change the representation of the system from the state-space representation to the dynamics governed by the linear Koopman operator on an infinite-dimensional space of observables. Whereas Koopman in his original paper dealt only with measure-preserving transformations, the discussion here is predominantly on dissipative systems arising from Navier-Stokes evolution. The analysis is based on spectral properties of the Koopman operator. Aspects of point and continuous parts of the spectrum are discussed. The point spectrum corresponds to isolated frequencies of oscillation present in the fluid flow, and also to growth rates of stable and unstable modes. The continuous part of the spectrum corresponds to chaotic motion on the attractor. A method of computation of the spectrum and the associated Koopman modes is discussed in terms of generalized Laplace analysis. When applied to a generic observable, this method uncovers the full point spectrum. A computational alternative is given by Arnoldi-type methods, leading to so-called dynamic mode decomposition, and I discuss the connection and differences between these two methods. A number of applications are reviewed in which decompositions of this type have been pursued. Koopman mode theory unifies and provides a rigorous background for a number of different concepts that have been advanced in fluid mechanics, including global mode analysis, triple decomposition, and dynamic mode decomposition.

1. INTRODUCTION

Proper orthogonal decomposition (POD): decomposition of a physical field, such as the velocity field, into spatial modes that are ranked by contributions to a quadratic or some other norm of the field

Fluid flows at high Reynolds number present us with a bewildering complexity of interactions that at times appear driven by organized structures and at times lack any detectable structure whatsoever. Researchers have long been striving to detangle this complexity by isolating features of flows that appear to have a dominant effect on the dynamics, such as localized vortices, as well as strain and shear structures (Batchelor 2000), with the idea that a certain superposition of dynamics driven by such structures will describe the flow accurately. Although these studies lead to important information about the dynamics of such coherent, isolated structures, the equations governing fluid-flow motion at high Reynolds number are nonlinear, and thus even the possibility of such superposition is called into question. The joint dynamics of coherent structures can be studied using statistical mechanics, as in Lundgren & Pointin (1977), using the assumption of ergodicity, to determine the long-term statistical properties or resulting flows. However, often our interest is not in the long-term properties, such as the average Eulerian velocity, but instead is in short-term, dynamical aspects, such as spatial and temporal properties of instability inception. An example in which much of the focus is on short-term, transient dynamics is the control of fluid flows (Koumoutsakos & Mezić 2006).

An idea that permeates applied mathematics, theoretical physics, and engineering for problems that deal with transient features is that of the expansion of a possibly complicated function of space and time into an infinite sum of simpler components. The most common such examples are of course the Taylor and Fourier expansions (or decompositions) and the more recent addition of wavelet decompositions (for applications in fluid dynamics, see Farge 1992). For these decompositions, a prefixed set of functions of space is chosen, and the evolving function or field is projected onto those to obtain time-dependent coefficients. We could call these decompositions with a predetermined basis. Another approach is the expansion into proper orthogonal modes, called proper orthogonal decomposition (POD) (Holmes et al. 1998), Karhunen-Loeve decomposition, or empirical orthogonal components decomposition, among other names. POD has been rediscovered a number of times since the initial works of Karhunen and Loeve in the context of stochastic processes. In comparison to the previous example of Taylor and Fourier expansions, in POD the spatial functions chosen to represent an evolving function (or a field) are dependent

PROPER ORTHOGONAL DECOMPOSITION

POD was introduced in fluid dynamics by Holmes, Lumley, and Berkooz (see Holmes et al. 1998), following the original work of Karhunen-Loeve, Lorenz, and others. The technique, as originally developed, aims to decompose a physical field (e.g., the velocity field) into a sum of spatially orthogonal modes defined on the flow domain. Its implementation requires knowledge of the time-averaged spatial correlation matrix of the velocity field. In the context of the Koopman operator ideas reviewed in this article, each spatial mode obtained by the POD procedure is a projection of the product of velocities at points x and y, $v(x)$ and $v(y)$ onto the eigenspace of the Koopman operator at eigenvalue 1 (recall that the eigenspace at 1 corresponds to fields that are time averages of observables). The resulting decomposition is closest to the original field in the least-squares sense (there are also variants that minimize other norms). Galerkin projection of the field on the resulting modes yields a system of ordinary differential equations. One of the most common uses for POD in fluid dynamics is the analysis of the flow physics using a truncated set of equations from the Galerkin projection. The known problems with this procedure are that the selection of modes that preserve stability properties of the original evolution can be sensitive (Amsallem & Farhat 2012). This is related to the fact that instabilities are dynamical events that start with modes of small energy.

on the evolution of the function itself. In fact, out of all orthogonal expansions that could represent the field, POD has the convenient property that it is the closest to the field at every finite expansion length, in a least-squares (or energy) sense. However, dynamical information is not always captured well. For example, very small energy perturbations can lead to a large-scale instability. Moreover, although POD mode decomposition would capture the high-energy consequences of such a perturbation, the initial small energy perturbation would not be featured as important.

An alternative concept has emerged in work of Mezić (2005), in which the author studied the problem of decomposing evolution of a field from the perspective of operator theory. The essence of the idea is to provide a decomposition that is based on projection onto eigenfunctions of a linear operator—the Koopman, or composition, operator—associated with the dynamical evolution of the underlying field. The technical aspects of this are described in Section 3. The approach is based not on the concept of the closeness of the projection to the full dynamics of the field, but instead on decomposition into dynamically relevant modes. These modes have the property that they represent the collective motion of fluid, in which a spatial shape is multiplied by a time-dependent function of form $\exp(\lambda t)$ for complex λ, which is an eigenvalue of the Koopman operator. (Time dependence can be more complicated in the case of degenerate eigenvalues.) In fact, the resulting decomposition in the case of a linear system is the decomposition into normal modes that proves useful in the theory of oscillations. Thus, by applying it, we achieve continuity in the treatment of linear and nonlinear dynamics.

The resulting modes—named Koopman modes by Rowley et al. (2009)—are not necessarily orthogonal. They are also a natural extension of the concept of global modes advocated in the 1990s by Huerre & Monkewitz (1990). These authors defined global modes as spatial structures that evolve at a single frequency. That concept was associated with linearization by Theofilis (2003) and Henningson & Åkervik (2008), but the work of Mezić (2005) proved rigorously that there is no need for that: Global modes, as defined by Huerre & Monkewitz (1990), are related to the point spectrum of the Koopman operator associated with the fully nonlinear evolution. In fact, as shown below, the more recent work showing how one can obtain global modes by solving an eigenvalue problem for perturbation around the mean (time-averaged) flow is yet another consequence of Koopman mode expansion (Pier 2002, Noack et al. 2003, Barkley 2006).

These concepts can also be connected to the work of Reynolds & Hussain (1972) on triple decomposition in which the flow is decomposed into its mean, periodically oscillating (coherent), and incoherent parts (in fact, this fluid mechanical connection was pointed out in Mezić 2005). This definition is valid for asymptotic evolution, in which transient evolution has subsided.

Here we define Koopman modes as the projection of an observable such as the velocity field on an eigenfunction of the Koopman operator. (Vorticity and pressure modes are of interest but have not been studied yet.) This definition subsumes the previous concepts and defines Koopman modes as collective motions of fluid that are occurring at the same spatial frequency, growth, or decay rate. The analysis becomes even more general when there are degenerate eigenvalues, and a more complex, collective time evolution that incorporates algebraic terms can be present. In addition, the existence of a continuous spectrum poses a largely open problem on how to represent that part of the flow in terms of structures that are local (but not associated with linearization) in time, frequency, and space but that also possess aspects of collective motion.

A numerical method for decomposing fluid flows named dynamic mode decomposition (DMD) was first proposed by Schmid & Sesterhenn (2008) and later published in Schmid (2010). Rowley et al. (2009) demonstrated that there is a relationship between Koopman mode decomposition and DMD and specifically that DMD modes constitute a subset of Koopman modes. The computation of DMD modes is based on an efficient group of algorithms from linear algebra, called

Koopman operator: an infinite-dimensional linear operator that evolves fields of physical observables defined on a state space of a dynamical system

Koopman mode: a spatial field defined on the domain of evolution of the physical observable (e.g., fluid-flow domain, on which the velocity field is defined) obtained by projection of the physical field onto an eigenvector of the Koopman operator

Global mode: a spatial mode of an observable field, such as the velocity field that oscillates at a single frequency and phase under the dynamical evolution of the field

Dynamic mode decomposition (DMD): a decomposition of a physical field obtained using modes obtained by the Arnoldi algorithm for finding eigenvalues and eigenvectors of linear operators

DYNAMIC MODE DECOMPOSITION

DMD was introduced in fluid mechanics by Schmidt & Sesterhenn (2008). It is based on considering the sequence of snapshots $v^0, v^1, \ldots v^N$ of a flow field. An assumption is made that the snapshots are related by a matrix A such that $v^{k+1} = Av^k$. The eigenvalues and eigenvectors of A are then found either through algorithmic implementation based on the full matrix or via consideration of the eigenvalues and eigenvectors of the companion matrix described in the text. In terms of Koopman operator-based analysis, the finite matrix A can be considered as a finite-dimensional approximation of the action of an infinite-dimensional operator, the Koopman operator, restricted to the Krylov subspace of flow fields spanned by the snapshots.

Arnoldi-type methods, based on snapshots of the dynamical evolution of observables (e.g., of fluid velocity) at regular time intervals. The combination of rigorous analysis in Mezić (2005) and efficient computational methods in Rowley et al. (2009) and Schmid (2010) has led to rapidly growing applications of this approach.

In this review, Section 2 discusses the treatment of fluid-flow velocity as a field of state-space observables, in which the state space is the space of Fourier coefficients associated with Galerkin projection onto a suitable basis of functions on the physical space. Section 3 defines and discusses a variety of properties of the Koopman operator, including its spectral properties. The notion of Koopman modes is defined, and the expansion of dynamics into the sum of such modes multiplied by suitable coefficients is discussed. A general rigorous method is introduced to compute Koopman modes called generalized Laplace analysis (GLA), and several examples of expansion are presented, including the harmonic oscillator, general linear systems, and nonlinear observables on a stable linear system. Koopman mode analysis is connected to global modes based on perturbation from the mean flow. Computation methods of Koopman modes based on Arnoldi-type algorithms are also reviewed. Section 5 reviews some applications of Koopman mode analysis to a variety of fluid flows and other dynamical processes. Section 6 concludes.

2. VELOCITY FIELD AS A FIELD OF STATE-SPACE OBSERVABLES

2.1. Galerkin Representation of Fluid Flow

For simplicity, the discussion in this section is restricted to incompressible flows. However, the ideas presented here, and the general Koopman spectrum–based analyses, are quite general and easily extendible to compressible flow and to multiphase flow situations.

The dynamics of incompressible fluid flow is most commonly studied using the Eulerian framework, via the nondimensional version of Navier-Stokes equations

$$\mathbf{u}_t + \mathbf{u} \cdot \nabla \mathbf{u} = -\nabla p + \frac{1}{Re}\nabla^2 \mathbf{u} + \mathbf{f}(\mathbf{x}), \quad \nabla \cdot \mathbf{u} = 0, \tag{1}$$

where $Re = \rho UL/\mu$ is the Reynolds number, U a characteristic velocity, L a length scale, and T a timescale. The nondimensional forcing $\mathbf{f}$ is assumed steady for simplicity. [Throughout, all vectors are written in bold font (e.g., $\mathbf{x}$), and their respective elements are written in standard font with indices as subscripts (e.g., $x_1, x_2, \ldots$). The subscript t (e.g., c_t) indicates partial differentiation with time, and ∇ is the gradient operator.] The density of the fluid is ρ and its viscosity μ. Velocity and pressure are nondimensional, with velocity scaled by U and pressure scaled by ρU^2. For simplicity, we assume periodic boundary conditions in a three-dimensional unit box and represent

$\mathbf{u}(\mathbf{x}, t)$ using spatial Fourier decomposition:

$$\mathbf{u}(\mathbf{x}, t) = \sum_{\mathbf{k}\in\mathbb{Z}^3} a_{\mathbf{k}}(t) \exp(i2\pi\mathbf{k}\cdot\mathbf{x}), \tag{2}$$

where as usual $i = \sqrt{-1}$ and $a_{-\mathbf{k}}(t) = a^c_{\mathbf{k}}(t)$ to obtain real vector $\mathbf{u}$, with $a^c_{\mathbf{k}}$ the complex conjugate of the coefficient $a_{\mathbf{k}}$. Then, using Galerkin projection, an infinite set of differential equations is obtained for $a_{\mathbf{k}}(t)$:

$$\dot{a}_{\mathbf{k}}(t) = f(\mathbf{a}_{\mathbf{k}}), \tag{3}$$

where $\mathbf{a}_{\mathbf{k}}$ is the infinite-dimensional vector of Fourier coefficients (see, e.g., Rowley et al. 2004). Famously, in many cases in which the existence and uniqueness of solutions are known, the dynamics settles on a finite-dimensional attractor (Temam 1997). Thus, at least when considering the dynamics on the attractor only, we are dealing with a finite (albeit possibly large) dimensional dynamical system.

2.2. Velocity Field as Field of State-Space Observables

The space A of coefficients $\mathbf{a}_{\mathbf{k}}$ can be thought of as the state space for fluid-flow evolution, and the velocity at every point $\mathbf{x}$ is a vector-valued function on that state space, as is evident from Equation 2. Namely, picking a point in A, $\mathbf{a}_{\mathbf{k}}$, we can obtain the vector $\mathbf{u}$ at any point $\mathbf{x}$:

$$\mathbf{u}(\mathbf{x}) = \sum_{\mathbf{k}\in\mathbb{Z}^3} a_{\mathbf{k}} \exp(i2\pi\mathbf{k}\cdot\mathbf{x}). \tag{4}$$

Thus we can think of $\mathbf{u}(\mathbf{x})$ as a family of vector-valued linear observables on A parameterized by $\mathbf{x}$. Specifically, the value of observable $\mathbf{u}(\mathbf{x})$ that the system sees at time t is given by Equation 2.

3. KOOPMAN OPERATOR, EIGENFUNCTIONS, AND MODES

3.1. Koopman Operator for Continuous-Time Dynamical Systems

For a general dynamical system

$$\dot{\mathbf{z}} = \mathbf{F}(\mathbf{z}), \tag{5}$$

STATE-SPACE REPRESENTATION OF PROBLEMS IN FLUID MECHANICS AND FIELDS OF OBSERVABLES

We give two familiar examples in which a state-space representation of fluid flow can be obtained in analytical form. The first stems from vortex dynamics. The position of a vortex moving inside a unit circle is described by the angle ϕ moving on a circular trajectory with constant radius. The evolution of ϕ is linear in time. The velocity field is a function of ϕ—the state-space variable, as well as the spatial (radial) coordinates at which the velocity is measured, r, θ. The evolution of the velocity field is periodic in time (Shashikanth & Newton 1998).

Another example stems from bifurcation theory. Rayleigh-Bénard convection can be studied using the Boussinesq approximation and in two-dimensional cases leads to two coupled partial differential equations for the stream function and temperature (Moehlis & Knobloch 2007). Just after the onset of convection, a state-space representation in the form of an amplitude equation $\dot{A} = a_1 A + a_3 A^3$ is derived, and observables ψ, the streamfunction, and θ, the temperature, are expressed as functions of A. The state-space equation for A can be linearized in the basin of attraction of its stable fixed point and transformed into $\dot{B} = -\lambda B$, an equation whose Koopman eigenfunctions we study below.

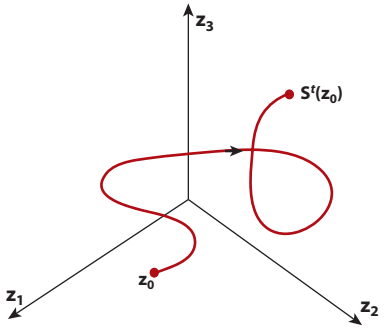

Figure 1

Trajectory of a dynamical system in $\mathbb{R}^3$.

defined on a state space A (i.e., $\mathbf{z} \in A$), where $\mathbf{z}$ is a vector and $\mathbf{F}$ is a possibly nonlinear vector-valued function, of the same dimension as its argument $\mathbf{z}$, we denote by $\mathbf{S}^t(\mathbf{z}_0)$ the position at time t of the trajectory of Equation 5 that starts at time zero at point $\mathbf{z}_0$ (see **Figure 1**).

We denote by $\mathbf{g}$ an arbitrary, vector-valued observable from A to $\mathbb{R}^m$. The value of this observable $\mathbf{g}$, which the system trajectory starting from $\mathbf{z}_0$ at time zero sees at time t, is

$$\mathbf{g}(t, \mathbf{z}_0) = \mathbf{g}(\mathbf{S}^t(\mathbf{z}_0)). \tag{6}$$

Note that the space of observables $\mathbf{g}$ is a vector space. The family of operators U^t, acting on the space of observables parameterized by time t, is defined by

$$U^t\mathbf{g}(\mathbf{z}_0) = \mathbf{g}(\mathbf{S}^t(\mathbf{z}_0)). \tag{7}$$

Thus, for a fixed τ, U^τ maps the vector-valued observable $\mathbf{g}(\mathbf{z}_0)$ to $\mathbf{g}(\tau, \mathbf{z}_0)$. With some abuse of language, we call the family of operators U^t the Koopman operator of the continuous-time system (Equation 5). This operator was defined for the first time in Koopman (1931) for Hamiltonian dynamical systems. In operator theory, such operators are often called composition operators, when defined for general dynamical systems, as U^t acts on observables by composing them with the mapping $\mathbf{S}^t$ (Singh & Manhas 1993).

3.2. Koopman Eigenfunctions

The operator U^t is linear, as can be easily seen from its definition (Equation 7); thus it makes sense to consider its spectral properties in the context of analyzing Equation 5. In this direction, we look for special observables $\phi(\mathbf{z}) : A \to \mathbb{C}$ on the state space that have the evolution in time given by

$$U^t\phi(\mathbf{z}_0) = \phi(\mathbf{S}^t(\mathbf{z}_0)) = \exp(\lambda t)\phi(\mathbf{z}_0). \tag{8}$$

Such observables (functions) ϕ are the eigenfunctions of U^t, and the associated numbers λ are the eigenvalues of U^t.

Example 1 (stable system in one dimension): Let us consider the following simple example of a stable dynamical system in one dimension,

$$\dot{z} = -\lambda z, \quad \lambda > 0. \tag{9}$$

The trajectories are given by $S^t(z_0) = z_0 \exp(-\lambda t)$. Let the observable $\varphi(z) = z$. We have

$$U^t\phi(z) = \phi(z\exp(-\lambda t)) = z\exp(-\lambda t) = \exp(-\lambda t)\phi(z),$$

and $\phi(z) = z$ is an eigenfunction of the Koopman operator associated with the eigenvalue $-\lambda$. This is the consequence of the more general property that for linear stable systems, the set of eigenvalues of the Koopman operator contains the spectrum of the system matrix (see Rowley et al. 2009 and below). However, the set of eigenvalues and eigenfunctions of the Koopman operator is larger than those "linear" ones, and it depends on the space of functions in which the evolution is taking place (Gaspard et al. 1995). Let us consider $\phi(z) = z^n$, $n \in \mathbb{Z}^+$. We have

Spectral expansion (decomposition): an expansion (decomposition) of a physical field into (generalized) eigenvectors of the Koopman operator

$$U^t\phi(z) = \phi(z\exp(-\lambda t)) = z^n \exp(-n\lambda t) = \exp(-n\lambda t)\phi(z),$$

and thus the functions $\phi(z) = z^n$ are eigenfunctions of U^t associated with eigenvalues $-n\lambda$. Despite the dynamics itself being linear, the eigenfunctions of the Koopman operator are not necessarily linear. These functions span the space of real-analytic functions on $\mathbb{R}$, and thus nonlinear observables evolving under linear dynamics can be represented by a spectral expansion using Koopman eigenfunctions. We consider then the evolution of any real-analytic observable $u(z)$, with Taylor expansion

$$u(z) = \sum_{j=0}^{\infty} u_j z^j,$$

where $u_j = (1/j!)d^j u/dz^j(0)$. Its evolution, given by $u(t, z) = U^t u(z)$, can be represented as

$$u(t, z) = U^t u(z) = U^t\left(\sum_{j=0}^{\infty} u_j z^j\right) = \sum_{j=0}^{\infty} u_j \exp(-j\lambda t)z^j.$$

For n real or negative, z^n is also an eigenfunction, provided we expand the space of observables in which we are interested. For example, if we allow in the space of observables functions that lack a derivative of order $[n] + 1$ (for real n, where $[n]$ is the integer part of n), n can be any real positive number. If n is negative, we need to allow for observables that have a singularity at zero.

We note that if ϕ_{λ_1} is an eigenfunction of U^t at λ_1 and ϕ_{λ_2} is an eigenfunction of U^t at λ_2, then $\phi_{\lambda_1} \cdot \phi_{\lambda_2}$ is an eigenfunction at $\lambda_1 + \lambda_2$:

$$\begin{aligned} U^t(\phi_{\lambda_1}(\mathbf{z})\phi_{\lambda_2}(\mathbf{z})) &= \phi_{\lambda_1}(S^t(\mathbf{z})) \cdot \phi_{\lambda_2}(S^t(\mathbf{z})) \\ &= \exp(\lambda_1 t)\phi_{\lambda_1}(\mathbf{z}) \exp(\lambda_2 t)\phi_{\lambda_2}(\mathbf{z}) \\ &= \exp((\lambda_1 + \lambda_2)t)\phi_{\lambda_1}(\mathbf{z})\phi_{\lambda_2}(\mathbf{z}). \end{aligned} \tag{10}$$

Thus, if we find an eigenvalue λ and the associated eigenfunction ϕ_λ, then $n\lambda$ is an eigenvalue for the associated eigenfunction ϕ_λ^n. It is easy to see how these results can be extended to diagonalizable linear systems of arbitrary dimension (Gaspard et al. 1995). In addition, a large class of nonlinear systems can be treated using a linearizing transformation, as shown in Gaspard et al. (1995) and Lan & Mezić (2012). Let us consider a nonlinear system $\dot{\mathbf{y}} = \mathbf{g}(\mathbf{y})$, within a basin of attraction of a fixed point or a limit cycle. If one can find an analytic linearizing transformation $\mathbf{z} = \mathbf{h}(\mathbf{y})$, then the spectrum of the Koopman operator of the nonlinear system is equal to that of the linear system. For the more general case of two conjugate systems, the reasoning is as follows: We let $\mathbf{S}^t$ and U_S^t be the family of mappings and the Koopman operator associated with $\dot{\mathbf{z}} = \mathbf{f}(\mathbf{z})$, and $\mathbf{T}^t$ and U_T^t be a family of mappings and the Koopman operator associated with $\dot{\mathbf{y}} = \mathbf{g}(\mathbf{y})$. Assume that $\phi(\mathbf{z})$ is an eigenfunction of U_S^t associated with eigenvalue λ. In addition, we let $\mathbf{h}$ be a mapping such that $\mathbf{S}^t(\mathbf{h}(\mathbf{y})) = \mathbf{h}(\mathbf{T}^t(\mathbf{y}))$; i.e., the two dynamical systems are conjugate. Then we have

$$\exp(\lambda t)\phi \circ \mathbf{h}(\mathbf{y}) = \phi(\mathbf{S}^t(\mathbf{h}(\mathbf{y}))) = \phi(\mathbf{h}(\mathbf{T}^t(\mathbf{y}))) = U_T^t(\phi \circ \mathbf{h}(\mathbf{y}));$$

i.e., if ϕ is an eigenfunction at λ of U_S^t, then the composition $\phi \circ \mathbf{h}$ is an eigenfunction of U_T^t at λ. In other words, if we can find a global conjugacy to a linear system or a skew-product of a linear system and rotation on a cycle [which was shown to be possible under general conditions in an entire basin of attraction of a fixed point or a limit cycle by Lan & Mezić (2012)], then the spectrum of the Koopman operator can be determined from the spectrum of the linearization at the fixed point or the limit cycle.

3.3. Koopman Modes

We assume now that we have a vector-valued observable $\mathbf{u}(\mathbf{z}, \mathbf{x})$, where $\mathbf{x} \in B \subset \mathbb{R}^n$ and $\mathbf{z} \in A$, the state space of the dynamical system (Equation 5).

Definition 1 (Koopman mode): The Koopman mode $\mathbf{s}(\mathbf{x})$ at isolated eigenvalue λ of algebraic multiplicity 1 is the projection of $\mathbf{u}(\mathbf{z}, \mathbf{x})$ onto the eigenfunction $\phi_\lambda(\mathbf{z})$ of U^t at λ.

The projection in question can be obtained as an inner product with the eigenfunction $\bar{\phi}_\lambda^c(\mathbf{z})$ at λ^c of the adjoint of U^t—the Perron-Frobenius operator (Gaspard 2005). This would, however, require an explicit calculation of such an eigenfunction. An alternative is provided by the following.

Theorem 1 (GLA): We let $\lambda_1, \ldots, \lambda_K$ be the eigenvalues of U^t such that $|\exp(\lambda_1)| \geq |\exp(\lambda_2)| \geq \cdots \geq |\exp(\lambda_K)|$. Then the Koopman mode associated with λ_K is obtained by computing

$$\phi_K(\mathbf{z})\mathbf{s}_K(\mathbf{x}) = \lim_{T\to\infty} \frac{1}{T} \int_0^T \exp(-\lambda_K t) \left[\mathbf{u}(S^t\mathbf{z}, \mathbf{x}) - \sum_{j=0}^{K-1} \exp(\lambda_j t)\phi_j(\mathbf{z})s_j(\mathbf{x}) \right] dt, \tag{11}$$

and we denote $\mathbf{s}_K(\mathbf{z}, \mathbf{x}) = \phi_K(\mathbf{z})\mathbf{s}_K(\mathbf{x})$.

Koopman modes are independent of initial conditions and, as shown in the example below, form a basis for the expansion of the evolution of the observable $\mathbf{u}$ starting from any initial condition in the state space (just as in the case of linear normal modes). The GLA computation starts by identifying or guessing the spectral radius (i.e., the largest Koopman eigenvalue associated with the evolution of the observable) and removing the contribution of that observable in the manner evident in Equation 11. However, this may lead to an unstable computation. An alternative is provided by the Arnoldi-type methods described below.

Example 2 (Koopman modes for a stable system): We consider now the field of observables on state space A parameterized by the spatial variable $x \in [0, 1]$, denoted by $u(z, x)$, evolving under the dynamics of Equation 9. The time evolution of this field is

$$u(t, z, x) = \sum_{j=0}^{\infty} \exp(-j\lambda t)z^j u_j(x),$$

where

$$u_j(x) = (1/j!)d^j u/dz^j(0, x)$$

is the Koopman mode associated with the eigenvalue $-\lambda_j = -j\lambda$. If we want to isolate the contribution to the time evolution of $u(z, x)$ that comes from a particular eigenvalue $K\lambda$, we use GLA. Let

$$\begin{aligned} s_K(z, x) &= \lim_{T\to\infty} \frac{1}{T} \int_0^T \exp(K\lambda t) \left[u(t, z, x) - \sum_{j=0}^{K-1} \exp(-j\lambda t)z^j u_j(x) \right] dt \\ &= \lim_{T\to\infty} \frac{1}{T} \int_0^T \exp(K\lambda t) \left[\sum_{j=K}^{\infty} \exp(-j\lambda t)z^j u_j(x) \right] dt \\ &= u_K(x)z^K. \end{aligned} \tag{12}$$

Note that (generalized) eigenfunctions of $(U^t)^T$—the Perron-Frobenius operator—are in this case given by the delta distribution and its derivatives $\delta^j(x)$, $j \in \mathbb{N}$, and $\int_A \delta^j(x)u(z,x)dz = \partial^j u/\partial z^j(0,x)$ (Gaspard et al. 1995). Thus the GLA provides the desired projection of $u(z,x)$ onto Koopman eigenfunctions obtained via the inner product with the dual eigenfunctions of the Perron-Frobenius operator.

In fact, for the case with no unstable modes,[1] and $|\exp(\lambda_K)| = 1$, the expression in Equation 11 reads (Mezić & Banaszuk 2004, Mezić 2005)

$$\mathbf{s}_K(\mathbf{z},\mathbf{x}) = \lim_{T\to\infty}\frac{1}{T}\int_0^T \exp(-\lambda_K t)u(S^t\mathbf{z},\mathbf{x})dt, \tag{13}$$

because all the other possible eigenvalues λ_j of U^t have $|\exp(\lambda_j)| \leq 1$, and those with $|\exp(\lambda_j)| = 1$ do not resonate with λ_K; i.e.,

$$\lim_{T\to\infty}\frac{1}{T}\int_0^T \exp(-\lambda_K t)\exp(\lambda_j t)dt = 0. \tag{14}$$

3.4. Spectral Expansion

Koopman modes are of interest because they are akin to the eigenvector expansions utilized in linear dynamics. In fact, in the case in which the system in Equation 5 is linear, and given by $\dot{\mathbf{z}} = \mathbf{A}\mathbf{z}$, its matrix eigenvalues are eigenvalues of the associated Koopman operator. The associated Koopman eigenfunctions are given by

$$\phi_j(\mathbf{z}) = \langle \mathbf{z}, \mathbf{w}_j\rangle, \quad j = 1,\ldots,n, \tag{15}$$

where $\mathbf{w}_j$ are eigenvectors of the adjoint $\mathbf{A}^*$ (that is, $\mathbf{A}^*\mathbf{w}_j = \lambda_j^c\mathbf{w}_j$), normalized so that $\langle \mathbf{v}_j, \mathbf{w}_k\rangle = \delta_{jk}$, where $\mathbf{v}_j$ is an eigenvector of $\mathbf{A}$, and $\langle\cdot,\cdot\rangle$ denotes an inner product on a linear space M in which the evolution is taking place (Rowley et al. 2009). This is easily seen by observing

$$\dot{\phi}_j = \langle \dot{\mathbf{z}}, \mathbf{w}_j\rangle = \langle A\mathbf{z}, \mathbf{w}_j\rangle = \langle \mathbf{z}, A^*\mathbf{w}_j\rangle = \lambda_j\langle \mathbf{z}, \mathbf{w}_j\rangle = \lambda_j\phi_j, \tag{16}$$

and thus

$$\phi_j(t,\mathbf{z}_0) = U^t\phi_j(\mathbf{z}_0) = \exp(\lambda_j t)\phi_j(\mathbf{z}_0).$$

Now, for any $\mathbf{z} \in M$, as long as $\mathbf{A}$ has a full set of eigenvectors at distinct eigenvalues λ_j, we may write

$$\begin{aligned}\mathbf{z} &= \sum_{j=1}^n \langle \mathbf{z}, \mathbf{w}_j\rangle\mathbf{v}_j = \sum_{j=1}^n \phi_j(\mathbf{z})\mathbf{v}_j,\\ U^t\mathbf{z}(\mathbf{z}_0) = \mathbf{z}(t) &= \sum_{j=1}^n \exp(\lambda_j t)\phi_j(\mathbf{z}_0)\mathbf{v}_j,\end{aligned} \tag{17}$$

where $\mathbf{z}(\mathbf{z}_0)$ is the vector function that associates Cartesian coordinates with a point $\mathbf{z}_0$ (the initial condition) in state space. Thus, for linear systems, the Koopman modes used in the expansion of $\mathbf{z}$ coincide with the eigenvectors of $\mathbf{A}$. Moreover, any nonlinear analytic observable can be expanded

[1] It is interesting that the theory allows for unstable modes, growing as $\exp(\lambda t)$, λ real and bigger than zero, if we allow for unbounded observables. The unstable modes feature prominently in linear stability theory. However, in the full nonlinear theory of Navier-Stokes equations, it is shown in a number of contexts (but not all!) that solutions are bounded. Thus the absence of unstable modes in Koopman spectrum computations is related to the fact that, over time, Navier-Stokes solutions settle on an attractor.

in the same way; we have done this in Example 2, using the products of eigenfunctions in the expansion.

Such analysis extends beyond linear systems. In the case of systems preserving measure μ, which includes the case in which we are studying the dynamics on the attractor of Navier-Stokes [with respect to the associated invariant physical measure on the attractor (Young 2002)], the complete spectral decomposition of a vector-valued function $\mathbf{g}(\mathbf{z}, \mathbf{x})$, where $\mathbf{z}$ is a state-space point and $\mathbf{x}$ is the point in the fluid domain, is given as

$$\begin{aligned} U^t\mathbf{g}(\mathbf{z},\mathbf{x}) &= U_s^t\mathbf{g}(\mathbf{z},\mathbf{x}) + U_r^t\mathbf{g}(\mathbf{z},\mathbf{x}) \\ &= \mathbf{g}^*(\mathbf{x}) + \sum_{j=1}^{k} \exp(\lambda_j t)\phi_j(\mathbf{z}) \int_M \mathbf{g}(\mathbf{z},\mathbf{x})\bar{\phi}_j(\mathbf{z})d\mu(\mathbf{z}) \\ &\quad + \int_0^1 \exp(i2\pi\alpha t)dE(\alpha)\mathbf{g}(\mathbf{z},\mathbf{x}) \\ &= \mathbf{g}^*(\mathbf{x}) + \sum_{j=1}^{k} \exp(\lambda_j t)\phi_j(\mathbf{z})\mathbf{s}_j(\mathbf{x}) + \int_0^1 \exp(i2\pi\alpha t)dE(\alpha)(\mathbf{g}(\mathbf{z},\mathbf{x})), \end{aligned}$$

where E is a complex, continuous spectral measure on L^2, which in the last part of the expansion represents the contribution from the continuous part of the spectrum, and U_s^t and U_r^t are operators on mutually orthogonal spaces of functions, where U_s^t has a pure point spectrum and U_r^t has a continuous spectrum (Plesner et al. 1969; see Mezić 2005 for the discrete-time version). It can be shown that the part corresponding to the point spectrum is an almost-periodic function in the sense of Bohr (Mezić 2005).

All the eigenvalues of the Koopman operator for a measure-preserving system are on the unit circle, and eigenfunctions of the Koopman operator are orthogonal (Petersen 1989, Mezić & Banaszuk 2004, Mezić 2005). Now the j-th Koopman mode reads

$$\mathbf{s}_j(\mathbf{x}) = \int_M \mathbf{g}(\bar{\mathbf{z}},\mathbf{x})\phi_j^c(\bar{\mathbf{z}})d\mu(\bar{\mathbf{z}}).$$

In this case, because of the orthogonality of eigenfunctions, the inner product is taken with the eigenfunction of the Koopman operator itself, in contrast to the general case described above in which the inner product involves eigenfunctions of the adjoint Perron-Frobenius operator. Note that, from Theorem 1, because all the eigenvalues of the expansion are of modulus 1, the Koopman mode at eigenvalue $i\omega_j$ can be obtained as

$$\phi_j(\mathbf{z})\mathbf{s}_j(\mathbf{x}) = \lim_{T\to\infty} \frac{1}{T}\int_0^T \exp(-i\omega t)\mathbf{u}(S^t\mathbf{z},\mathbf{x})dt. \tag{18}$$

Here we do not need to subtract the already computed part of the field from the data because all the eigenvalues have the same modulus. As pointed out by Wiener (1930) in his classic generalized harmonic analysis, Schuster (1897) already knew that harmonic averages such as Equation 18 can be applied to uncover hidden periodicities in signals.

The composite picture that develops from the above considerations is that the following triple decomposition of the velocity field arises from the spectral properties of the Koopman operator on the attractor:

$$\mathbf{u}(t,\mathbf{z},\mathbf{x}) = \mathbf{u}^*(\mathbf{z},\mathbf{x}) + \mathbf{u}_{ap}(t,\mathbf{z},\mathbf{x}) + \mathbf{u}_c(t,\mathbf{z},\mathbf{x}),$$

where $\mathbf{u}^*(\mathbf{z},\mathbf{x})$ is the time-averaged part of the field, $\mathbf{u}_{ap}(t,\mathbf{z},\mathbf{x})$ is almost periodic in time, and $\mathbf{u}_c(t,\mathbf{z},\mathbf{x})$ is the part of the field that is genuinely aperiodic (or chaotic) in time. Thus this part could be modeled as a stochastic process. This stochastic process can be expanded into Karhunen-Loeve modes in space (POD) (see Holmes et al. 1998). In fact, because the modal dynamics of

the POD in this case has a continuous spectrum, one could expect that the dynamics might be hyperbolic. The finite-dimensional truncations should have good structural stability properties in this case. An alternative to this decomposition of the continuous spectrum is the use of the so-called Ruelle-Pollicott resonances, which govern the relaxation of the chaotic part of the field, thus providing the coarse-grained picture of the continuous spectrum (Ruelle 1986, Cvitanović et al. 2005).

A direct association between various types of attractors studied in dynamical systems and the above decomposition can be drawn: Quasi-periodic attractors correspond to decomposition $\mathbf{u}(t, \mathbf{z}, \mathbf{x}) = \mathbf{u}^*(\mathbf{z}, \mathbf{x}) + \mathbf{u}_{ap}(t, \mathbf{z}, \mathbf{x})$; skew-periodic attractors, discussed in Broer & Takens (1993), correspond to decomposition $\mathbf{u}^*(\mathbf{z}, \mathbf{x}) + \mathbf{u}_{ap}(t, \mathbf{z}, \mathbf{x}) + \mathbf{u}_c(t, \mathbf{z}, \mathbf{x})$; and axiom A attractors (Young 2002) correspond to decomposition $\mathbf{u}^*(\mathbf{z}, \mathbf{x}) + \mathbf{u}_c(t, \mathbf{z}, \mathbf{x})$.

Example 3 (harmonic oscillator): In this example, we study the case in which the state-space dynamics is provided by a harmonic oscillator. Here $z = (z_1, z_2)$ and

$$\dot{z}_1 = z_2,$$

$$\dot{z}_2 = -\omega^2 z_1.$$

This system is divergence free and thus preserves area in state space. Thus it falls into the category of measure-preserving systems. The solution to this set of equations is given by

$$z_1(t) = \frac{\dot{z}_{20}(0)}{\omega}\sin(\omega t) + z_1(0)\cos(\omega t),$$
$$z_2(t) = \dot{z}_{20}(0)\cos(\omega t) - z_1(0)\omega\sin(\omega t).$$

We use the generalized Laplace transform, for the case $\lambda_{1,2} = \mp i\omega$, to project the observable's vector $(z_1(t), z_2(t))$(with $\mathbf{x} = \{1, 2\}$ as the index set or parameterizing variable) onto modes oscillating at a single frequency:

$$\lim_{T\to\infty}\frac{1}{T}\int_0^T \exp(\pm i\omega t)\begin{pmatrix} z_1(t) \\ z_2(t)\end{pmatrix} dt = \frac{1}{2}\begin{pmatrix} z_{10} \pm i z_{20}/\omega \\ z_{20} \mp i\omega z_{10}\end{pmatrix}. \tag{19}$$

The first projection is

$$\mathbf{s}_1(\mathbf{z}_0) = \frac{1}{2}\left[\begin{pmatrix} z_{10} \\ z_{20}\end{pmatrix} + i\begin{pmatrix} z_{20}/\omega \\ -\omega z_{10}\end{pmatrix}\right], \tag{20}$$

and the second one is its complex conjugate

$$\mathbf{s}_2(\mathbf{z}_0) = \frac{1}{2}\left[\begin{pmatrix} z_{10} \\ z_{20}\end{pmatrix} - i\begin{pmatrix} z_{20}/\omega \\ -\omega z_{10}\end{pmatrix}\right]. \tag{21}$$

We note that these projections play the role of functions $\mathbf{s}_i(\mathbf{z}, \mathbf{x})$ in the general theory. Because we are in a finite-dimensional context, the parameterizing set is such that x takes values in the finite set $\{1, 2\}$, and thus we just have vectors of two components $\mathbf{s}_i = \mathbf{s}(\mathbf{z}_{0;i})$, $i = 1, 2$.

Now we have

$$(z_1, z_2)^T = \mathbf{x} = \exp(-i\omega t)\mathbf{s}_1(\mathbf{z}_0) + \exp(i\omega t)\mathbf{s}_2(\mathbf{z}_0) = \exp(-i\omega t)A\mathbf{s}_1 + \exp(i\omega t)B\mathbf{s}_2, \tag{22}$$

where

$$\mathbf{s}_1 = \begin{pmatrix} 1 \\ -i\omega\end{pmatrix}, \tag{23}$$

and $\mathbf{s}_2$ is the complex conjugate $\mathbf{s}_1^c$ of $\mathbf{s}_1$, $A = 1/2(z_{10} + iz_{20}/\omega)$, and $B = A^c$. We can also check that $A(z_{10}, z_{20})$ is an eigenfunction of the Koopman operator of Equation 19 (and thus B as well,

as it is the complex conjugate of A by putting it in polar form): We let $r_0 = \sqrt{z_{10}^2 + (z_{20}/\omega)^2}$ and $\tan\theta = -z_{20}/(\omega z_{10})$. Because r_0 is an eigenfunction at eigenvalue zero (it is constant on the ellipse of invariant energy) and $\exp(\pm i\theta_0)$ is an eigenfunction associated with eigenvalue $\exp(\pm i\omega t)$, and because the product of eigenfunctions is an eigenfunction at the sum of eigenvalues, we get the form of the spectral expansion we derived in the general case of measure-preserving systems.

3.5. Relationship Between Koopman Modes and Mean-Flow-Based Global Modes

It is interesting to connect the expansion in Equation 18 with global mode analysis (described originally in Huerre & Monkewitz 1990) executed in the form of the analysis of perturbation around the mean (time-averaged) flow, as studied by Pier (2002), Noack et al. (2003), and Barkley (2006). For example, Barkley (2006) studied the Kármán vortex street in a wake of a two-dimensional circular cylinder. A perturbation equation was derived around the time-averaged flow velocity profile for the case of flow oscillating at a single frequency ω, and the solution of the associated eigenvalue problem yields an oscillation frequency such that the relationship between the Strouhal number based on that frequency and the Reynolds number matches experimental data extremely accurately. Such analysis is based on a certain assumption about the behavior of the Reynolds stress term.

To examine the validity of that procedure, we consider the time evolution of Equation 5. Assume that the dynamics settles on a limit cycle, yielding, from Equation 18,

$$\mathbf{z}(t) = \mathbf{z}^* + \sum_{n\in\mathbb{Z}/0} \exp(in\omega t)\mathbf{s}_n,$$

where $\mathbf{z}^*$ is the time average, and we omit the dependence of $\mathbf{s}_n$ on initial conditions, which is just the phase on the limit cycle. We obtain

$$\dot{\mathbf{z}} = \sum_{n\in\mathbb{Z}/0} in\omega \exp(in\omega t)\mathbf{s}_n = \mathbf{F}\left(\mathbf{z}^* + \sum_{n\in\mathbb{Z}/0} \exp(in\omega t)\mathbf{s}_n\right), \tag{24}$$

where the right-hand side is assumed to be an analytic function. Owing to its periodicity in t, it admits the Fourier expansion

$$\mathbf{F}\left[\mathbf{z}^* + \sum_{n\in\mathbb{Z}/0} \exp(in\omega t)\mathbf{s}_n\right] = \sum_{n\in\mathbb{Z}/0} \exp(in\omega t)\mathbf{F}_n,$$

where

$$\mathbf{F}_n = \frac{1}{T}\int_0^T \mathbf{F}\left[\mathbf{z}^* + \sum_{n\in\mathbb{Z}/0} \exp(in\omega t)\mathbf{s}_n\right] \exp(-in\omega t)dt. \tag{25}$$

Now, because of the analyticity of $\mathbf{F}$, we expand into a Taylor series around $\mathbf{z}^*$ and consider the case $n = 1$:

$$\mathbf{F}_1 = \frac{1}{T}\int_0^T \left[\mathbf{F}(\mathbf{z}^*) + \sum_{n\in\mathbb{Z}/0} \exp(in\omega t)\nabla\mathbf{F}(\mathbf{z}^*)\cdot\mathbf{s}_n + H.O.T.\right] \exp(-i\omega t)dt. \tag{26}$$

There are at least two different situations in which the higher-order terms (*H.O.T.*) in Equation 26 can be neglected: (*a*) when the $\mathbf{s}_n$ are small and (*b*) when the dynamics on the limit cycle is harmonic, and subharmonics can be neglected. Note that the Galerkin projection (Equation

3) has a quadratic right-hand side, and thus the third- and higher-order derivatives in Equation 26 are zero. In these cases, the only oscillatory terms that survive the integration are $n = \pm 1$. Using Equations 24–26, we obtain

$$i\omega \mathbf{s}_1 = \nabla \mathbf{F}(\mathbf{z}^*) \cdot \mathbf{s}_1,$$

and the Koopman mode $\mathbf{s}_1$ is the solution of the global mode eigenvalue problem, which is in a fluid mechanical context obtained as a perturbation around the mean (time-averaged) flow.

The expansion in Equation 18 was derived for the first time in Mezić (2005), for the case of discrete-time dynamical systems. When one considers dissipative systems, with stable and unstable directions to the attractor, the spaces of functions need to be changed (Gaspard et al. 1995). For example, in the case in which the attractor is a limit cycle, a function space to work with can be $L^2(S^1) \times \mathcal{A}(S^1)^\perp$, where $\mathcal{A}(S^1)^\perp$ is the space of analytic functions that do not depend on the variable θ describing the position along the limit cycle, as shown by Y. Lan & I. Mezić (unpublished manuscript).

4. COMPUTATION OF KOOPMAN MODES

Koopman modes in principle can be computed directly using GLA, presented in Theorem 1. In the case of $|\exp(\lambda)| = 1$, this reduces to Fourier analysis. Fast Fourier transform can be used to find the spectrum associated with an observable. Peaks of that spectrum are then identified, and the harmonic average can be computed using Equation 13. The caveat here is that different observables in principle will present different spectra, so the whole Koopman spectrum and its modes might not be revealed. In theory, the spectrum for a generic observable contains the full spectrum of the Koopman operator, but even the first examples computed show that there is a significant difference in the spectra of different observables (e.g., velocities calculated or observed at two different and distant points in the flow field). **Figure 2** shows the time traces of two observables—streamwise velocities at two different points in space, one near the wall and another near the jet. The Koopman spectrum revealed by the Arnoldi-type algorithm for Koopman eigenvalue computation (Rowley et al. 2009), discussed below, is richer than the spectra of either observable. In the numerical simulation of fluid flows, some papers plot the eigenvalue $\exp(\lambda)$ inside the unit circle, as done in Rowley et al. (2009). Owing to the discrete nature of the simulations performed, a discrete sequence $U^{n\Delta t}, n = 0, \ldots, N$ is obtained. Thus, if λ is an eigenvalue of U^t with mode $\mathbf{s}(\mathbf{z}, \mathbf{x})$, then the obtained evolution associated with that mode is $\alpha^n \mathbf{s}(\mathbf{z}, \mathbf{x}) = \exp(n\lambda\Delta t)\mathbf{s}(\mathbf{z}, \mathbf{x})$, yielding $\log_e \alpha = \lambda\Delta t$, and the eigenvalue is plotted at $\exp[(\log_e \alpha)/\Delta t]$. As an example, **Figure 3** shows the numerically computed Koopman eigenvalues and the two strongest oscillatory Koopman modes corresponding to Koopman eigenvalues on the unit circle (i.e., on the attractor) of the jet in transverse flow—the first case for which Koopman modes were computed (Rowley et al. 2009).

In principle, one can find the full spectrum of the Koopman operator by performing GLA, in which Equation 3 is used on some function $g(\mathbf{z})$ starting from the unit circle, successively subtracting parts of the signal corresponding to eigenvalues with decreasing $|\lambda|$. In practice, such computation can be unstable, as at large t it involves multiplication of a very large number with a very small number. Also, although a generic observable will reveal all the eigenvalues of the Koopman operator, it is easy to find examples, such as the harmonic oscillator example above, in which the use of specific observables reveals only a portion of the spectrum. In the harmonic oscillator example, we chose the states x_1 and x_2 as observables. As these are linear observables, and the system itself is linear, the only eigenvalues revealed by GLA were $\pm i\omega$. For a generic nonlinear observable, the eigenvalues would be $in\omega, n \in \mathbb{Z}$. Rowley et al. (2009) proposed the use of an Arnoldi-type algorithm to compute Koopman modes. Prior to that, Schmid & Sesterhenn

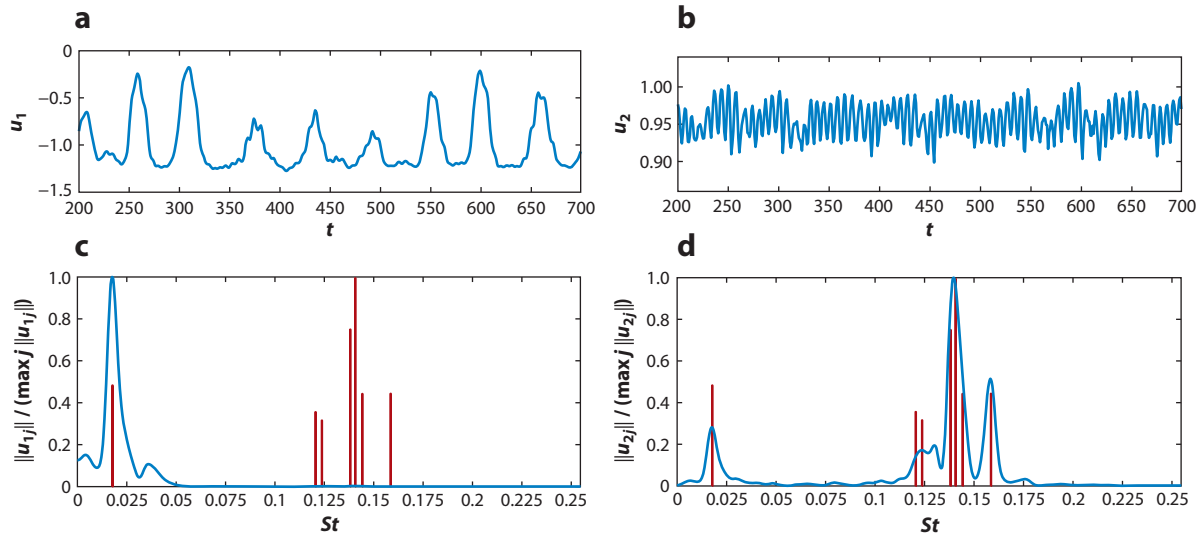

Figure 2

(*a*,*b*) The velocity signal (*a*) near the wall and (*b*) near the jet. (*c*,*d*) Part of the spectrum of the Koopman operator for a jet in transverse flow computed by the Arnoldi method (*red*) and the spectrum associated with the velocity signal (*blue*) for the cases shown in panels *a* and *b*. The Strouhal number *St* is plotted on the horizontal axis, and the normalized mode magnitude is plotted on the vertical axis. Figure taken from Rowley et al. (2009).

(2008) proposed the use of an Arnoldi algorithm in computing the DMD (the published version is Schmid 2010). The version of the Arnoldi algorithm derived by Ruhe (1984) and applied by Rowley et al. (2009) and Schmid (2010) computes eigenvalues based on the so-called companion matrix. More precisely, if $\mathbf{u}_j \in \mathbb{R}^n$, $j = 0, \ldots, m$ is a sequence of fluid velocity snapshots at times $j\Delta t$ (where n is the number of spatial points at which the velocity is obtained), the companion matrix is defined as

$$C = \begin{bmatrix} 0 & 0 & \cdots & 0 & c_0 \\ 1 & 0 & & 0 & c_1 \\ 0 & 1 & & 0 & c_2 \\ \vdots & & \ddots & & \vdots \\ 0 & 0 & \cdots & 1 & c_{m-1} \end{bmatrix}, \tag{27}$$

where $c_1, i = 1, \ldots m-1$ are such that

$$\mathbf{u}_m = \sum_{j=1}^{m-1} c_i \mathbf{u}_i + \mathbf{r},$$

and $\mathbf{r}$ is the residual vector that is zero provided $\mathbf{u}_m$ can be obtained as a linear combination of $\mathbf{u}_1, \ldots, \mathbf{u}_{m-1}$ (which certainly happens when $m > n$). For $m \leq n$, if $\mathbf{u}_m$ cannot be expressed as a linear combination of previous snapshots, the residual vector $\mathbf{r}$ is chosen to be orthogonal to the subspace spanned by $\mathbf{u}_1, \ldots, \mathbf{u}_{m-1}$. In the context of discrete-time dynamical systems (as obtained from numerical simulation or experimental data), defined on state space A by

$$\mathbf{z}' = T(\mathbf{z}),$$

and observable $f: A \to \mathbb{R}$, the time evolution under T yields the sequence of observables $\{f(\mathbf{z}), f(T^2(\mathbf{z})), \ldots, f(T^{m-1})(\mathbf{z}), \ldots\} = \{f_0, f_1, \ldots, f_{m-1}, \ldots\}$. The left shift operator on this

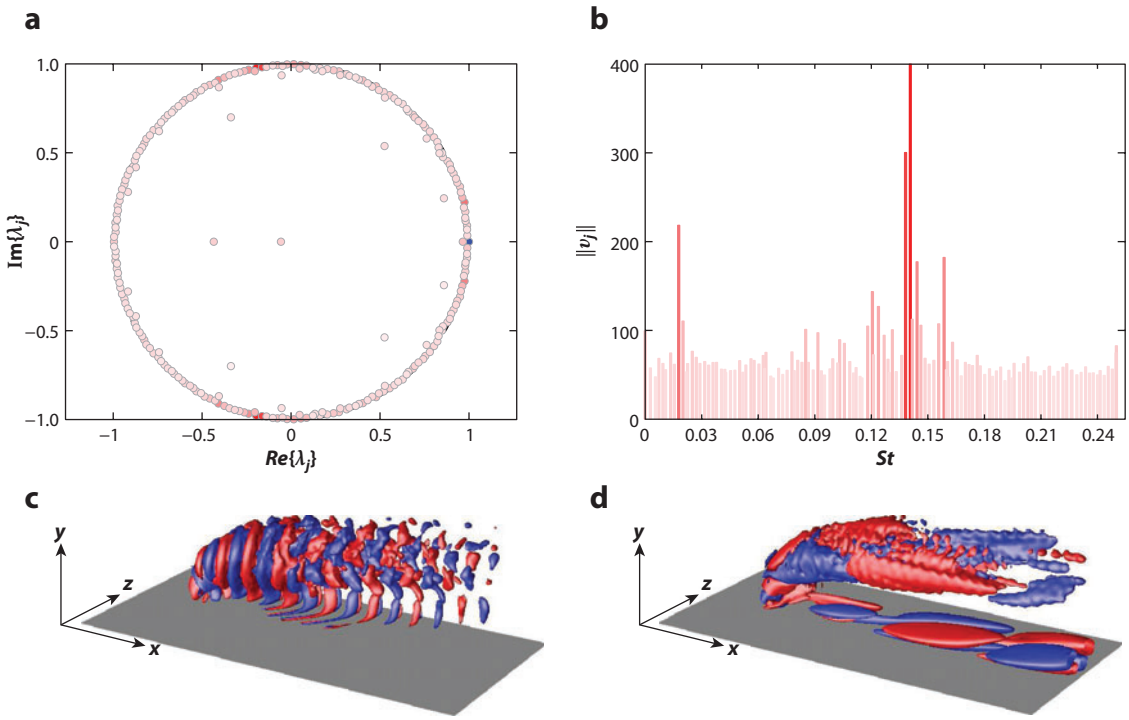

Figure 3

(*a*,*b*) Part of the spectrum of the Koopman operator for a jet in crossflow, with (*a*) Koopman eigenvalues on the unit circle, with the darker red indicating a larger Koopman mode amplitude and blue indicating eigenvalue 1, and (*b*) their magnitudes. (*c*,*d*) The two largest magnitude Koopman modes corresponding to (*c*) high and (*d*) low frequency. Positive (*red*) and negative (*blue*) contour levels of the streamwise velocity components of two Koopman modes are shown. The direction of the crossflow is *z*. Figure taken from Rowley et al. (2009).

sequence is defined by

$$S(\{f_0, f_1, \ldots, f_{m-1}, \ldots\}) = \{f_1, f_2, \ldots, f_m, \ldots\}$$

and has a matrix representation in an infinite-dimensional companion matrix

$$C = \begin{bmatrix} 0 & 0 & \cdots & 0 & 0 \\ 1 & 0 & & 0 & 0 \\ 0 & 1 & & 0 & 0 \\ \vdots & & \ddots & & \vdots \end{bmatrix}. \tag{28}$$

Thus the spectrum of the Koopman operator restricted to the subspace spanned by $\mathbf{u}(T^n(\mathbf{z}), \mathbf{x})$ is equal to the spectrum of the infinite-dimensional companion matrix, and the associated Koopman modes are given by $\mathbf{Ka}$ (provided that $\mathbf{a}$ does not belong to the null space of $\mathbf{K}$), where

$$\mathbf{K} = [\mathbf{u}_0 \mathbf{u}_1 \ldots \mathbf{u}_{m-1} \ldots]$$

is the column matrix (vector-valued if $\mathbf{u}$ contains all three velocity components) of velocity snapshots at times $0, \Delta t, \ldots, (m-1)\Delta t, \ldots$, and $\mathbf{a}$ is an eigenvector of the shift operator restricted to Krylov subspace spanned by $\mathbf{u}_i$. In this sense, the finite-dimensional companion matrix in

Equation 27 can be thought of as an approximation to the action of the Koopman operator on the associated finite-dimensional Krylov subspace.

Chen et al. (2012) proved that the decomposition (eigenvalues and modes) obtained from the DMD approach is unique, provided that eigenvalues are isolated and snapshots of the flow are independent. They also observed that subtracting the mean of the sequence of snapshots leads to all possible eigenvalues being on the unit circle, the companion matrix analysis reducing essentially to the discrete Fourier transform. However, the problem with subtraction of the mean is in fact related to the observation above that the companion matrix is an approximation to the Koopman operator representation on a finite-dimensional set of functions. When the mean $\mathbf{u}^* = \sum_{j=0}^{m} \mathbf{u}_j/(m+1)$ is subtracted from the finite sequence of snapshots to obtain the new sequence $\{\mathbf{u}_0 - \mathbf{u}^*, \mathbf{u}_1 - \mathbf{u}^*, \ldots, \mathbf{u}_m - \mathbf{u}^*\}$, the action of the Koopman operator on this sequence is not represented by the shift but can be written as

$$\{\mathbf{u}_0 - \mathbf{u}^*, \mathbf{u}_1 - \mathbf{u}^*, \ldots \mathbf{u}_m - \mathbf{u}^*\} \to \left\{\mathbf{u}_1 - \mathbf{u}^* + \frac{1}{m+1}(\mathbf{u}_0 - \mathbf{u}_{m+1}),\right.$$
$$\mathbf{u}_2 - \mathbf{u}^* + \frac{1}{m+1}(\mathbf{u}_0 - \mathbf{u}_{m+1}),$$
$$\left.\ldots, \mathbf{u}_m - \mathbf{u}^* + \frac{1}{m+1}(\mathbf{u}_0 - \mathbf{u}_{m+1})\right\}.$$

When $m \to \infty$, the above transformation has a limit that is the action of the Koopman operator, but this is not so for any finite m, except when the specific periodicity on the attractor is such that $\mathbf{u}_0 = \mathbf{u}_m$. In that case, as Chen et al. (2012) demonstrated, the DMD computation reduces to a discrete Fourier transform. This is in line with a statement in Mezić (2005) that on-attractor (quasi-)periodicities can be computed using the so-called harmonic averages, which are the special case of GLA when $|\lambda| = 1$. However, in general, the computation of Koopman modes by the DMD method needs to be done without subtracting the mean if decaying or growing modes are to be captured.

In addition, Chen et al. (2012) devised an optimized version of the DMD algorithm, in which, instead of a residual error at the last snapshot, they allow for errors at all snapshots but optimize the eigenvalues to fit the data. They performed the analysis of error incurred by truncating the mode set and found that the harmonic average (corresponding to the method proposed in Mezić 2005) and optimized DMD modes perform equally and also better than any other modes tested. However, DMD and optimized DMD algorithms capture the eigenvalues and modes relatively well, even with a short time sequence of snapshots (much shorter than the inherent period of the flow), whereas harmonic averages do not. Thus, computationally, there is an interesting space-time tradeoff for the two methods. Koopman eigenvalues and the value of Koopman modes at a spatial point can be captured by GLA provided one has even a single point but also a long time trace of data. Conversely, DMD methods based on Arnoldi-type algorithms seem to be able to capture Koopman eigenvalues and Koopman modes over a shorter period from data that have a larger spatial extent. The global-mode-type analysis discussed above is also a promising computational method for the Koopman spectrum and mode computation, and it would be interesting to develop it further.

5. APPLICATIONS OF KOOPMAN MODE ANALYSIS

The realization that the DMD algorithm computes Koopman eigenvalues and—via the calculation of the inverse of the so-called truncated Vandermonde matrix (see Bagheri 2010)—a subset of

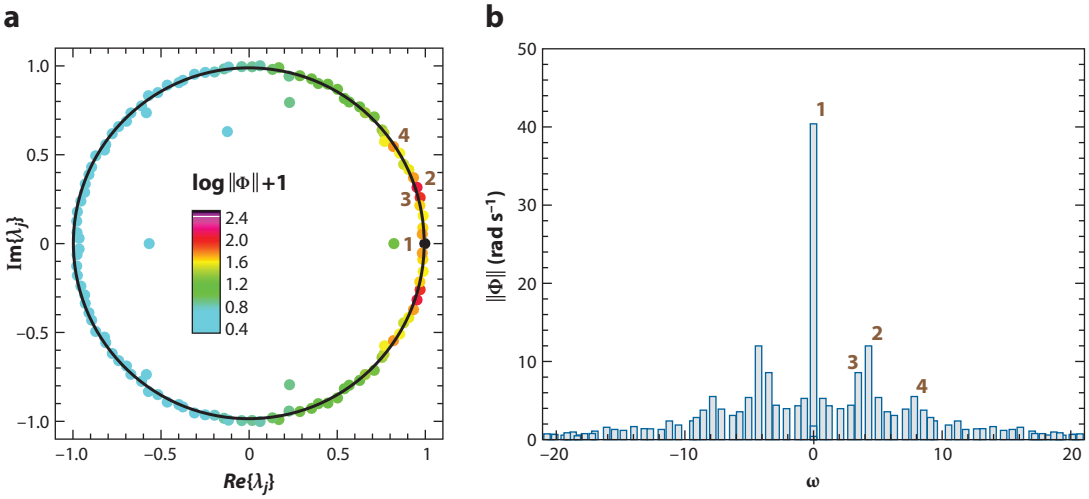

Figure 4

Part of the spectrum of the Koopman operator for self-sustained oscillations in turbulent cavity flow, with (*a*) Koopman eigenvalues on the unit circle and (*b*) their magnitudes plotted against frequency ω in radians per second. Figure taken from Seena & Sung (2011).

Koopman modes[2] led to its application in a variety of contexts. Henningson (2010) briefly summarized the state of knowledge up to that point. It is evident from the description below that the number of works using the concepts of Koopman modes and the DMD algorithm is growing rapidly.

Tammisola et al. (2011) studied the stability of viscous confined-plane wakes and established a connection of the so-called global linear mode theory with Koopman mode analysis, in their case using essentially the Fourier version of GLA. By performing a careful comparison of spectra obtained from linear stability analysis and nonlinear investigations in which the associated Koopman modes are found, they concluded that although linear stability analysis correctly predicts the initial nonlinear behavior and therefore the stability boundary, the nonlinear state is different for the Reynolds numbers toward the end of the range investigated. Specifically, the frequency of nonlinear (Koopman) modes can differ by as much as 10% from the linear frequency.

Seena & Sung (2011) used Koopman modes to study self-sustained oscillations in turbulent cavity flows. Eigenvalues of the Koopman operator for a Reynolds number of 12,000, at which self-sustained oscillations were present, show a clear indication of oscillatory Koopman modes (for eigenvalues 1–4 in **Figure 4**). Two different cases were studied using the DMD algorithm. In the case of thick boundary layers, Koopman modes associated with the upcoming boundary layer and shear layer structures had coincident frequencies but different spatial wave numbers. No self-sustained oscillations were found. In the case of a thin incoming boundary layer, these structures have the same temporal frequencies and spatial wave numbers, indicating coupling between two spatial domains and ensuing internal resonance. Seena & Sung pointed out the differences in the Koopman spectrum when sampling a subdomain of a flow versus the full domain. This is related to the theoretical discussion above. When a subdomain is sampled, a smaller vector of observables is evolving in time, and the spectrum of such a small vector of observables can be a subset of the spectrum observed in the full domain. This is evident from figures 8 and 10 in Seena & Sung (2011).

[2] More precisely, the resulting vectors are $\mathbf{s}(\mathbf{z}, \mathbf{x})$, as defined in this article. Koopman modes do not depend on initial conditions. The modes obtained by Arnoldi algorithm do.

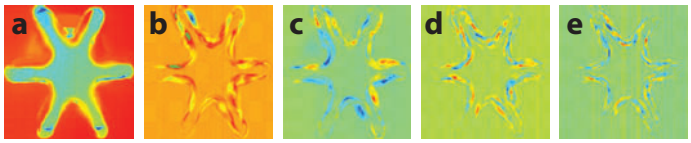

Figure 5

Top five Koopman modes of a jet emanating from the lobe diffuser, with increasing frequency from left to right, indicating how an increase in frequency oscillations leads to higher-wave-number spatial oscillations of the modes. Figure taken from Nastase et al. (2011).

Nastase et al. (2011) studied Koopman modes in lobed jets emanating from three-dimensional diffusers for HVAC applications. **Figure 5** shows the top five Koopman modes, with increasing oscillation frequency from left to right. Higher-frequency temporal oscillations in this case correspond to higher spatial wave-number oscillations of the corresponding modes. They used the DMD algorithm to extract the dominant Koopman modes and, with this analysis, confirmed their hypothesis that the dominant mode is related to Kelvin-Helmholtz structures at the lobe trough.

Schmid et al. (2011) applied the DMD algorithm to schlieren snapshots of a helium jet and to time-resolved particle image velocimetry (PIV) measurements of an unforced and harmonically forced jet. As shown in the middle panel of **Figure 6**, the eigenvalues are presented in a different format than in Rowley et al. (2009) and Seena & Sung (2011): The frequency is in hertz, $\mathrm{Im}(\lambda_i)/(2\pi)$ is on the horizontal axis, and the decay rate $Re(\lambda_i)$ is on the vertical axis. The emphasis in the current review article is on the abstract concept of the field of observables and their projections on the eigenfunctions of the Koopman operator. Schmid et al. (2011) confirmed the physical relevance of such projections for two very different fields of observables: schlieren snapshots and PIV measurements. The authors analyzed the spatial structure of Koopman modes and concluded that the primary effect of forcing is concentrated near the nozzle exit, where oscillatory vortical fluid elements are introduced that dominate the forced dynamics. For the unforced jet, the decomposition shows a more typical behavior characterized by the progressive roll-up of the outer shear layer in the downstream direction.

Tu et al. (2011) studied the separated flow over a finite-thickness flat plate at $Re = 100{,}000$ in which the flow is characterized by up to three distinct natural frequencies: those of the shear layer, separation bubble, and wake. They computed the POD and Koopman modes and compared the two approaches. When the separation point is moved near the trailing edge, there are Koopman modes that have support in the shear layer and in the far wake, and such modes are absent from POD analysis, suggesting that these Koopman modes indicate the interaction between the shear layer and the wake. The analysis of a forced (controlled) flow and the resulting Koopman modes was pursued, revealing that the effectiveness of the control strategy resides in enhancing the shear layer–wake interaction modes.

Duke et al. (2012) investigated highly resolved velocity measurements of the interfacial velocity of an aerodynamically driven annular liquid sheet. Based on unstable Koopman mode analysis, they proposed that two distinct instability sources are present, rather than one, and measured their growth rates for the first time.

A number of applications of Koopman mode analysis are emerging in different fields as well. For example, Susuki & Mezić used it to study coherency in power grids (Susuki & Mezić 2009) and to study precursors to the so-called swing instability in the power-grid context (Susuki & Mezić 2011), whereas Eisenhower et al. (2010) studied the dynamics of energy data and models of buildings using Koopman modes.

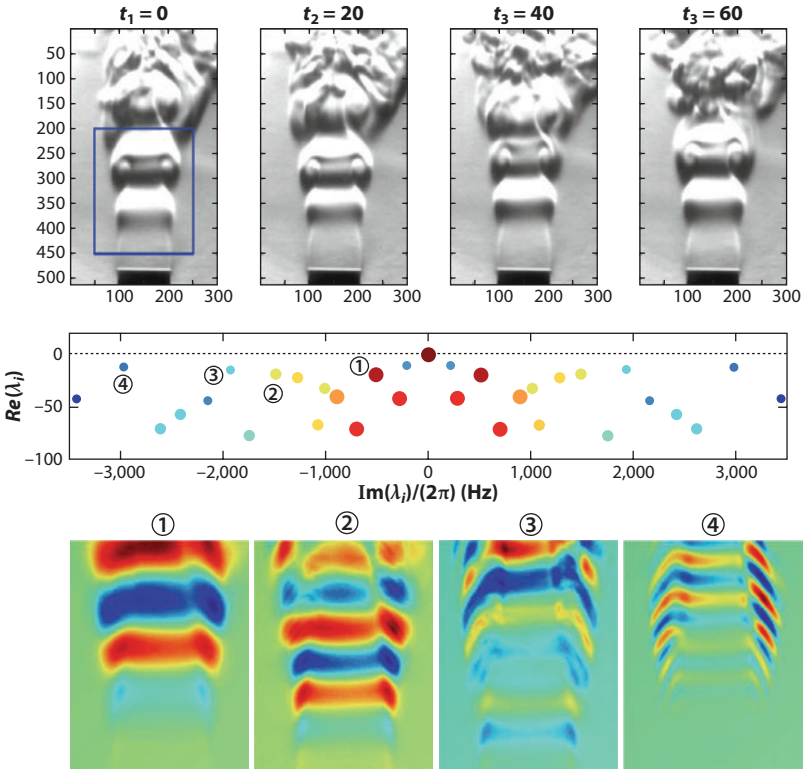

Figure 6

(*Top panel*) Time evolution of a low-density helium jet. (*Middle panel*) Koopman spectrum obtained using an Arnoldi algorithm. Larger symbols correspond to larger-scale structures, and smaller ones to smaller-scale structures. (*Bottom panel*) Four Koopman modes, whose eigenvalues are numbered in the middle panel. Figure taken from Schmid et al. (2011).

6. DISCUSSION AND CONCLUSIONS

In this review of the theory and applications of Koopman modes, we encounter a variety of ideas and concepts in fluid mechanics that have been proposed and used to obtain collective motions of fluid in the fully nonlinear regime, missing a common theoretical underpinning. Such concepts, discussed above, are the global modes, triple decomposition, and DMD. The concept of Koopman modes, derived from spectral properties of the infinite-dimensional, linear, Koopman operator associated with a (linear or nonlinear) dynamical system, provides a unified theoretical background for these concepts. In practice, the Koopman operator does not have to be realized to obtain the modes. Indeed, the methods of computation of Koopman modes such as GLA and DMD deal with snapshot sequences of the velocity field, whereas global mode analysis relies on the linearization around the mean velocity field profile. This fact also enables these methods to be applied to PIV, schlieren, and other fields obtained from experimental measurement.

The method for extracting Koopman modes, as deployed so far in fluid mechanics, is good for flows with strong peaks in the spectrum, but flows with a broad spectrum need further resolution, as shown, for example, by Muld et al. (2012), who compared POD and Koopman modes for the flow around a surface-mounted cube that possibly has a continuous spectrum and did not find

much difference between the two modes. In fact, Mezić (2005) argued that POD could be a robust method for decomposition of the continuous-spectrum part of the flow, and it is interesting that the two approaches (Koopman and POD decomposition) in practice yield similar results for such flows. To understand such flows, progress is needed on the theoretical front, by unraveling further mysteries of the Koopman operator structure.

SUMMARY POINTS

1. An overview is presented of the theory and applications of fluid-flow decompositions based on spectral properties of the Koopman operator—a linear, infinite-dimensional operator associated with the dynamical systems governing the flow evolution. The notion of Koopman eigenfunctions and Koopman modes is reviewed.
2. The relationship between a variety of theoretical concepts and Koopman modes is discussed. Global modes, dynamic mode decomposition, and triple decomposition all have their theoretical justification within the spectral theory of the Koopman operator.
3. Numerical analysis of Koopman modes is largely based on methods of dynamic mode decomposition, although Fourier-transform-based methods are available for modes associated with the dynamics on the attractor.
4. The applications of Koopman operator–based analysis include the detection of coherent structures in incompressible and compressible flows, global stability analysis, and the unraveling of the interaction of flow structures in different parts of the flow domain (e.g., the interaction of the shear layer and far wake in the case of the separated flow over a finite-thickness plate), as well as the analysis of forced (controlled) flows.

FUTURE ISSUES

1. Whereas the Koopman spectrum–based modal decomposition of systems with quasi-periodic dynamics is well understood, the representation of systems with a mixed (part-point, part-continuous) spectrum lacks sufficient theoretical understanding.
2. As discussed above, Arnoldi-type methods provide a finite-dimensional representation of the Koopman operator action on a Krylov subspace. An understanding of errors inherent in such an approximation should be enabled by that realization.
3. The Laplace transform–based methods for computing Koopman modes have well-known error estimates. For example, the convergence in the case of a quasi-periodic attractor (e.g., a limit cycle), where the method commonly used is the fast Fourier transform, is given by $1/N$ where N is the number of snapshots. However, noisy data and problems with spectrum estimation can make that approach deteriorate. Can advanced methods from signal processing be used and further developed to enable this method of computation? Can a method be designed that utilizes the theory in generalized Laplace analysis but does not suffer from the numerical issues present when stable and unstable modes are being computed?
4. How effective are the Koopman spectrum–based decompositions applied to vorticity and pressure fields?

DISCLOSURE STATEMENT

The author is not aware of any biases that might be perceived as affecting the objectivity of this review.

ACKNOWLEDGMENTS

This work was partially supported by AFOSR grant FA9550-10-1-0143 (Program Manager Dr. Fariba Fahroo) and ARO grant W911NF-11-1-0511 (Program Manager Dr. Samuel Stanton). I am very thankful for their support. I am thankful to Dr. Bryan Eisenhower and Dr. Alexandre Mauroy, as well as Dr. Marko Budišić and Mr. Ryan Mohr for their critical reading of the manuscript and many good suggestions.

LITERATURE CITED

Amsallem D, Farhat C. 2012. Stabilization of projection-based reduced-order models. *Int. J. Numer. Methods Eng.* 91:358–77

Bagheri S. 2010. *Analysis and control of transitional shear flows using global modes*. PhD diss. Dep. Mech., R. Inst. Technol.

Barkley D. 2006. Linear analysis of the cylinder wake mean flow. *Europhys. Lett.* 75:750–56

Batchelor GK. 2000. *An Introduction to Fluid Dynamics*. Cambridge, UK: Cambridge Univ. Press

Broer H, Takens F. 1993. Mixed spectra and rotational symmetry. *Arch. Ration. Mech. Anal.* 124:13–42

Chen KK, Tu JH, Rowley CW. 2012. Variants of dynamic mode decomposition: connections between Koopman and Fourier analyses. *J. Nonlinear Sci.* In press

Cvitanović P, Artuso R, Mainieri R, Tanner G, Vattay G. 2005. *Chaos: Classical and Quantum*. **http://www.chaosbook.org**

Duke D, Honnery D, Soria J. 2012. Experimental investigation of nonlinear instabilities in annular liquid sheets. *J. Fluid Mech.* 691:594–604

Eisenhower B, Maile T, Fischer M, Mezić I. 2010. *Decomposing building system data for model validation and analysis using the Koopman operator*. Presented at Int. Build. Perform. Simul. Assoc. SimBuild Conf., New York

Farge M. 1992. Wavelet transforms and their applications to turbulence. *Annu. Rev. Fluid Mech.* 24:395–458

Gaspard P. 2005. *Chaos, Scattering and Statistical Mechanics*. Cambridge, UK: Cambridge Univ. Press

Gaspard P, Nicolis G, Provata A, Tasaki S. 1995. Spectral signature of the pitchfork bifurcation: Liouville equation approach. *Phys. Rev. E* 51:74–94

Henningson D. 2010. Description of complex flow behaviour using global dynamic modes. *J. Fluid Mech.* 656:1–4

Henningson DS, Åkervik E. 2008. The use of global modes to understand transition and perform flow control. *Phys. Fluids* 20:031302

Holmes P, Lumley JL, Berkooz G. 1998. *Turbulence, Coherent Structures, Dynamical Systems and Symmetry*. Cambridge, UK: Cambridge Univ. Press

Huerre P, Monkewitz PA. 1990. Local and global instabilities in spatially developing flows. *Annu. Rev. Fluid Mech.* 22:473–537

Koopman BO. 1931. Hamiltonian systems and transformation in Hilbert space. *Proc. Natl. Acad. Sci. USA* 17:315–18

Koumoutsakos PD, Mezić I. 2006. *Control of Fluid Flow*. Berlin: Springer-Verlag

Lan Y, Mezić I. 2012. Linearization at large of nonlinear systems. *Physica D*. Manuscript submitted

Lundgren TS, Pointin YB. 1977. Statistical mechanics of two-dimensional vortices. *J. Stat. Phys.* 17:323–55

Mezić I. 2005. Spectral properties of dynamical systems, model reduction and decompositions. *Nonlinear Dyn.* 41:309–25

Mezić I, Banaszuk A. 2004. Comparison of systems with complex behavior. *Physica D* 197:101–33

Moehlis J, Knobloch E. 2007. Equivariant dynamical systems. *Scholarpedia* 2(10):2510

Provides a good comparison of the different global mode techniques.

Discovered that the spectral decomposition of the Koopman operator associated with a dynamical system evolving a spatial field leads to the definition of global spatial modes that oscillate at a single frequency.

Muld TW, Efraimsson G, Henningson DS. 2012. Mode decomposition on surface-mounted cube. *Flow Turbul. Combust.* 88:279–310

Nastase I, Meslem A, El Hassan M. 2011. Image processing analysis of vortex dynamics of lobed jets from three-dimensional diffusers. *Fluid Dyn. Res.* 43:065502

Noack BR, Afanasiev K, Morzynski M, Tadmor G, Thiele F. 2003. A hierarchy of low-dimensional models for the transient and post-transient cylinder wake. *J. Fluid Mech.* 497:335–63

Petersen K. 1989. *Ergodic Theory*. Cambridge, UK: Cambridge Univ. Press

Pier B. 2002. On the frequency selection of finite-amplitude vortex shedding in the cylinder wake. *J. Fluid Mech.* 458:407–17

Plesner AI, Nestell MK, Gibbs AG. 1969. *Spectral Theory of Linear Operators*. New York: Ungar

Reynolds WC, Hussain A. 1972. The mechanics of an organized wave in turbulent shear flow. Part 3. Theoretical models and comparisons with experiments. *J. Fluid Mech.* 54:263–88

Rowley CW, Colonius T, Murray RM. 2004. Model reduction for compressible flows using POD and Galerkin projection. *Physica D* 189:115–29

Rowley CW, Mezić I, Bagheri S, Schlatter P, Henningson DS. 2009. Spectral analysis of nonlinear flows. *J. Fluid Mech.* 641:115–27

Ruelle D. 1986. Resonances of chaotic dynamical systems. *Phys. Rev. Lett.* 56:405–7

Ruhe A. 1984. Rational Krylov sequence methods for eigenvalue computation. *Linear Algebra Appl.* 58:391–405

Schmid PJ. 2010. Dynamic mode decomposition of numerical and experimental data. *J. Fluid Mech.* 656:5–28

Schmid PJ, Li L, Juniper MP, Pust O. 2011. Applications of the dynamic mode decomposition. *Theor. Comput. Fluid Dyn.* 25:249–59

Schmid P, Sesterhenn J. 2008. Dynamic mode decomposition of numerical and experimental data. *Bull. Am. Phys. Soc.* 53:102

Schuster A. 1897. On lunar and solar periodicities of earthquakes. *Proc. R. Soc. Lond.* 61:455–65

Seena A, Sung HJ. 2011. Dynamic mode decomposition of turbulent cavity flows for self-sustained oscillations. *Int. J. Heat Fluid Flow* 32:1098–110

Shashikanth BN, Newton PK. 1998. Vortex motion and the geometric phase. Part I. Basic configurations and asymptotics. *J. Nonlinear Sci.* 8:183–214

Singh RK, Manhas JS. 1993. *Composition Operators on Function Spaces*. North-Holl. Math. Stud. 179. Amsterdam: North Holland

Susuki Y, Mezić I. 2009. Nonlinear Koopman modes and coherency identification of coupled swing dynamics. *IEEE Trans. Power Syst.* 26:1894–904

Susuki Y, Mezić I. 2012. Nonlinear Koopman modes and a precursor to power system swing instabilities. *IEEE Trans. Power Syst.* 27:1182–91

Tammisola O, Lundell F, Schlatter P, Wehrfritz A, Söderberg LD. 2011. Global linear and nonlinear stability of viscous confined plane wakes with co-flow. *J. Fluid Mech.* 675:397–434

Temam R. 1997. *Infinite-Dimensional Dynamical Systems in Mechanics and Physics.* Appl. Math. Sci. 68. New York: Springer-Verlag

Theofilis V. 2003. Advances in global linear instability analysis of nonparallel and three-dimensional flows. *Prog. Aerosp. Sci.* 39:249–316

Tu JH, Rowley CW, Aram E, Mittal R. 2011. *Koopman spectral analysis of separated flow over a finite-thickness flat plate with elliptical leading edge*. Presented at AIAA Aerosp. Sci. Meet. New Horiz. Forum Aerosp. Expo., 49th, Orlando, FL, AIAA Pap. 2011-38

Wiener N. 1930. Generalized harmonic analysis. *Acta Math.* 55:117–258

Young LS. 2002. What are SRB measures, and which dynamical systems have them? *J. Stat. Phys.* 108:733–54

Demonstrated that the Arnoldi-type method proposed by Schmid & Sesterhenn (2008) produces approximations to Koopman modes.

Provides the first written exposition of the DMD as devised by Schmid.

Presents an Arnoldi-type method for the decomposition of fluid flows, leading to the realization in Rowley et al. (2009) that such methods identify Koopman modes.

Presents a method from which precursors to global instabilities can be identified.

Demonstrates the first use of Koopman mode analysis to study controlled flows.